

NIH RELAIS Document Delivery

NIH-10286767

JEFFDUYN

NIH -- W1 J0795E

JOZEF DUYN
10 Center Dirve
Bldg. 10/Rm.1L07
Bethesda, MD 20892-1150

ATTN: SUBMITTED: 2002-08-29 17:22:16
PHONE: 301-594-7305 PRINTED: 2002-09-04 07:15:09
FAX: - REQUEST NO.: NIH-10286767
E-MAIL: SENT VIA: LOAN DOC
7967404

NIH	Fiche to Paper	Journal
-----	----------------	---------

TITLE: JOURNAL OF NEUROSURGERY
PUBLISHER/PLACE: American Association of Neurological Sur
Charlottesville, VA :
VOLUME/ISSUE/PAGES: 1997 Oct;87(4):516-24 516-24
DATE: 1997
AUTHOR OF ARTICLE: Tedeschi G; Lundbom N; Raman R; Bonavita S; Duyn JH;
Alger J
TITLE OF ARTICLE: Increased choline signal coinciding with malignant
ISSN: 0022-3085
OTHER NOS/LETTERS: Library reports holding volume or year
0253357
9322842
SOURCE: PubMed
CALL NUMBER: W1 J0795E
REQUESTER INFO: JEFFDUYN
DELIVERY: E-mail: jhd@helix.nih.gov
REPLY: Mail:

NOTICE: THIS MATERIAL MAY BE PROTECTED BY COPYRIGHT LAW (TITLE 17, U.S. CODE)

---National-Institutes-of-Health,-Bethesda,-MD-----

Increased choline signal coinciding with malignant degeneration of cerebral gliomas: a serial proton magnetic resonance spectroscopy imaging study

GIOACCHINO TEDESCHI, M.D., NINA LUNDBOM, M.D., PH.D., RAMESH RAMAN, M.D., SIMONA BONAVIDA, M.D., JEFF H. DUYN, PH.D., JEFFREY R. ALGER, PH.D., AND GIOVANNI DI CHIRO, M.D.

Neuroimaging Branch, National Institute of Neurological Disorders and Stroke, and Laboratory of Diagnostic Radiology Research, National Institutes of Health, Bethesda, Maryland; and Department of Radiological Sciences, Brain Research Institute, Johnson Comprehensive Cancer Center, University of California, Los Angeles, California

✓ The authors tested the hypothesis that proton magnetic resonance spectroscopy (¹H-MRS) imaging can be used as a supportive diagnostic tool to differentiate clinically stable brain tumors from those progressing as a result of low- to high-grade malignant transformation or posttherapeutic recurrence. Twenty-seven patients with cerebral gliomas verified on histological examination were studied repeatedly with ¹H-MRS imaging over a period of 3.5 years. At the time of each ¹H-MRS imaging study, clinical examination, MR imaging, positron emission tomography with ¹⁸F-fluorodeoxyglucose, and biopsy findings (when available) were used to categorize each patient as having either stable or progressive disease. Measures of the percentage changes in the choline (Cho) ¹H-MRS imaging signal intensity between studies, which were obtained without knowledge of the clinical categorization, allowed the investigators to segregate the groups with a high degree of statistical significance. All progressive cases showed a Cho signal increase between studies of more than 45%, whereas all stable cases showed an elevation of less than 35%, no change, or even a decreased signal. The authors conclude that increased Cho levels coincide with malignant degeneration of cerebral gliomas and therefore may possibly be used as a supportive indicator of progression of these neoplasms.

KEY WORDS • primary brain tumor • cerebral glioma • malignant degeneration • tumor recurrence • magnetic resonance spectroscopy • proton magnetic resonance spectroscopy imaging • choline

THE clinical challenge of managing primary brain tumors is still quite formidable.^{3,28,31,33,41,49,51} The need for prompt and accurate recognition of a low- to high-grade progression and/or of a posttherapeutic recurrence in cerebral gliomas has given impetus to continued reassessment and to the search for novel neuroimaging methods. Although computerized tomography (CT) and magnetic resonance (MR) imaging can solve many diagnostic problems related to brain tumors, they do not provide the biological information critical to the appropriate management of cerebral gliomas.^{29,57} Positron emission tomography with ¹⁸F-fluorodeoxyglucose (FDG-PET) provides insights into tumor cell metabolism and has emerged as a powerful method to assess the biological behavior of cerebral gliomas.^{1,9-11,13-15,17,18,22-26,32,39,40,45,47,56} However, the fact that PET facilities are available in only a few specialized centers has severely limited the widespread adoption of the FDG-PET method to manage cerebral gliomas. The wider availability of single photon emission CT (SPECT) scanners has intensified the search for SPECT tracers suitable to evaluate gliomas. Views of

the proposed radionuclide alternatives (PET and SPECT) are available in the literature.^{4,12,20}

In contrast to the scarcity of PET equipment and its ancillary services, high-field (1.5- and 2-tesla) MR imaging devices are found in most medical centers and enable proton magnetic resonance spectroscopy (¹H-MRS) and its variant ¹H-MRS imaging to be performed. Recently, a large number of reports describing both ¹H-MRS^{2,3,7,21,30,37,38,42,50,55} and ¹H-MRS imaging^{6,19,43,48} have indicated that this technique offers biological information about brain tumors. Of particular interest is the report by Preul, et al.,⁴³ who presented data indicating that ¹H-MRS imaging can assist in determining the histopathological type of brain tumor. Other studies contain preliminary data on the application of ¹H-MRS imaging to monitor therapy for such neoplasms.^{6,19} It is apparent that ¹H-MRS imaging may offer supportive evidence to identify deterioration caused by recurrence or malignant degeneration.

In this study we tested the hypothesis that serial ¹H-MRS imaging can help detect malignant degeneration and/or the recurrence of brain gliomas. We refer to these

two related phenomena as "progression." This hypothesis is based on our previous observations of individual cases,¹⁹ which indicate that the choline (Cho) signal increases with tumor progression. At the time of the repeated ¹H-MRS imaging examinations, patients were categorized with either stable or progressive disease, based on the preponderance of information derived from the neurological examination, MR imaging, FDG-PET scanning, and histological studies (in the majority of the patients with progressive disease). Our aim was to evaluate if the change in Cho signal intensity relative to the most recent ¹H-MRS imaging study could segregate progressive from stable cases.

Clinical Material and Methods

Neuroimaging Studies

We used multisection ¹H-MRS imaging, which allows simultaneous acquisition of spectral signal intensities from four 15-mm sections divided into a number of 0.84-ml single-volume elements.¹⁶ The acquired data can be displayed in a tomographic format, thus making ¹H-MRS imaging particularly suitable to explore the metabolic heterogeneity of intracranial tumors.^{6,19,37,43,48} The ¹H-MRS imaging method allows us to recognize several endogenous brain chemicals.^{27,46} The principal metabolite signals in the long echo time ¹H-MRS imaging are from *N*-acetyl-containing compounds (*N*-acetyl aspartate [NAA] as the prominent contributor); Cho-containing compounds; creatine plus phosphocreatine (CR); and lactate (LAC). Among the chemicals detected by ¹H-MRS imaging, Cho is likely to be the most reliable indicator of malignancy in human gliomas. The elevated Cho signal probably reflects an increase in metabolites that are precursors of the membrane phospholipids needed to support neoplastic proliferation, as well as compounds involved in the rapid cellular turnover.^{2,6,19,37,43,48}

The multisection (four-slice) ¹H-MRS imaging studies were performed with a 1.5-tesla MR imager equipped with self-shielded gradients using an established data acquisition procedure.¹⁶ Phase encoding was used to obtain a 32 × 32-element array of spectra from voxels having a nominal volume of 0.84 ml (7.5 × 7.5 × 15 mm) within the selected slices. The ¹H-MRS imaging data acquisition comprised a multiple-slice spin-echo slice selection with a repetition time of 2300 msec and an echo time of 272 msec. Outer-volume signal saturation was used to suppress signals arising from the skull marrow and surface tissues. Four 15-mm-thick slices with 3-mm interslice spacing were acquired. After completing the ¹H-MRS imaging, a series of T₂-weighted images were obtained with the same field of view and oblique angulation used for the ¹H-MRS image acquisition. Contiguous slicing (3-mm thickness) was used so that a total of five 3-mm images from the MR series corresponded to any single 15-mm ¹H-MRS imaging slice.

The ¹H-MRS imaging reconstruction was performed on a SPARC-II workstation (Sun Microsystems Computer Corp., Mountain View, CA) using specially designed software. The data sets, which were reconstructed one slice at a time, were zero-filled to 32 × 32 spatial and 512 time domain elements. The spatial dimensions were filtered

with a sine function and the time dimension was filtered with a 2-Hz exponential filter. Fourier transformation in all three dimensions resulted in a 32 × 32-element array of spectra. To facilitate rapid automatic processing, further calculations were performed with magnitude-corrected spectral data. Signal intensity images were produced by determining the signal within 0.2 ± 0.1 ppm of the expected location of the NAA, Cho, CR, or LAC signals. Spectroscopic voxels showing poor spectral resolution (less than half-height separation of Cho and CR signals) or residual water and/or lipid signals were excluded.

Tumor regions of interest (ROIs) containing at least two spectroscopic voxels (7.5 × 7.5 × 15 mm) were selected from each study to include the area of highest Cho signal within the region exhibiting elevated T₂ weighting. In those cases in which no such area could be identified on the ¹H-MRS images, the tumor ROIs were selected from the T₂-weighted images. To calibrate the signal intensities from different imaging studies and individuals to a common scale, the signal amplitude of each metabolite (NAA, Cho, CR, and LAC) in the tumor ROI was normalized to the corresponding amplitude in matching ROIs from a normal area of the contralateral brain. Metabolite signal intensity ratios (NAA/Cho, NAA/CR, Cho/CR) were also calculated for each ROI.

A routine MR contrast study was performed in each patient separately within 2 days (before or after) of the ¹H-MRS imaging examination. The FDG-PET images were obtained according to well-established procedures.¹¹

Study Protocol

All patients were studied by using a protocol approved by the National Institutes of Health and informed consent was obtained from each participant before inclusion in the study. Twenty-seven patients who were referred for neuroimaging evaluation of verified cerebral gliomas participated. Over a period of 3.5 years, the 27 patients were tested 72 times. The clinicopathological features of the tumors, intervals from previous treatment to the time of the imaging studies, and the results of these studies (MR, FDG-PET, and ¹H-MRS imaging) are reported in Tables 1 (patients with stable disease) and 2 (patients with progressive disease). The clinical, MR imaging, and FDG-PET findings are presented as differences from the previous study. The ¹H-MRS imaging findings are presented both as individual study values and as between-studies percentage changes in normalized Cho.

In all patients the initial diagnosis was formulated from a histopathological examination of tissue specimens obtained from biopsy procedures. In most cases these evaluations were performed at other institutions prior to referral. An experienced neurologist (R.R.), who was unaware of the ¹H-MRS imaging results, categorized the cases as being stable (16 patients) or progressive (11 patients) at the time of each ¹H-MRS imaging examination. All patients classified with stable disease presented with unchanged clinical status since the previous examination. The patients with progressive disease showed either malignant degeneration of an untreated low-grade lesion or recurrence of a previously treated tumor. The categorization of the patients was based on the 45 repeated studies, and the first examination was used as the baseline. All

TABLE 1

Pathological, clinical, and neuroradiological findings in 16 patients with stable disease*

Case No.	Age (yrs), Sex	Diagnosis	Mos to Disease Onset	Mos to Treatment	Clinical Data	MR Imaging	FDG-PET	Cho on ¹ H-MRS Imaging	% Change Cho
1	65, M	astro III	95	95 (Sx & RT)	†	N	hypo	0.61	5
			112	11 (Sx & RT)	S	S, N	S, hypo	0.64	
2	36, M	astro II	4	4 (RT)	†	N	hypo	1.45	-3
			8	8 (RT)	S	S, N	S, hypo	1.40	
			11	11 (RT)	S	S, N	S, hypo	1.42	
			14	14 (RT)	S	S, N	S, hypo	1.44	
			29	29 (RT)	S	S, N	S, hypo	1.36	
3	37, F	astro III	28		†	N	hypo	1.59	15
			58		S	S, N	S, hypo	1.35	
4	32, M	astro II	15		†	N	hypo	0.85	11
			18		S	S, N	S, hypo	0.94	
			24		S	S, N	S, hypo	0.87	
			31		S	S, N	S, hypo	1.05	
			45		S	S, N	S, hypo	1.15	
5	62, M	astro II	144	60 (RT)	†	N	hypo	1.42	4
			150		S	S, N	S, hypo	1.47	
6	41, F	astro II	32		†	N	hypo	1.54	-1
			45		S	S, N	S, hypo	1.53	
			51		S	S, N	S, hypo	1.65	
			64		S	S, N	S, hypo	1.39	
7	37, M	astro II	12	12 (RT)	†	N	hypo	1.87	-5
			19	19 (RT)	S	S, N	S, hypo	1.77	
			25	25 (RT)	S	S, N	S, hypo	1.80	
8	63, F	astro II	204	120 (RT)	†	E	hypo	1.09	-33
			211	211 (RT)	S	S, E	S, hypo	0.72	
9	57, M	astro II	29		†	N	hypo	1.44	-3
			35	24 (Sx)	S	S, N	S, hypo	1.40	
			43		S	S	S, hypo	1.74	
10	35, F	astro II	71	71 (Sx)	†	E	hypo	0.61	7
			81	81 (Sx)	S	S, E	hypo	0.65	
			99	99 (Sx)	S	S, E	hypo	0.68	
11	43, M	astro III	22	2 (Sx, RT, & C)	†	E	hypo	0.81	5
			26		S	S, E	hypo	0.72	
			30		S	S, E	hypo	0.83	
			34		S	S, E	hypo	0.98	
12	44, M	astro III	32	32 (RT)	†	E	hypo	1.58	-1
			38		S	S, E	hypo	1.56	
			56		S	S, E	hypo	1.77	
			63		S	S, E	hypo	1.43	
			77		†	E	hypo	1.37	
13	61, F	astro II	90		S	S, E	S, hypo	1.21	-12
			104		S	S	S, hypo	1.06	
					†	N	hypo	2.02	
14	34, F	astro III	16		†	N	hypo	2.00	-1
			22		S	S, N	S, hypo	2.00	
15	58, M	oligo III	40	38 (Sx & RT)	†	E	hyper	1.58	-4
			46	44 (Sx & RT)	S	S	S, hyper	2.51	
16	40, M	astro III	60	1 (Sx)	†	E	hyper	2.18	-22
			70	11 (Sx & RT)	I	I	I, hyper	1.69	

* Astro = astrocytoma; C = chemotherapy; E = enhancing; hyper = hyperintense; hypo = hypointense; I = improved; N = nonenhancing; oligo = oligodendroglioma; RT = radiotherapy; S = stable; Sx = surgery.
 † No comparison with radiological studies was performed at baseline.

available data at the time of the repeated examination, such as neurological examination, MR imaging, FDG-PET, and biopsy results were used to categorize the patients. In the progressive group, a malignant transformation was proven on biopsy studies in seven of the 11 cases.

The time from onset of disease to imaging was 48.5 ± 40.9 months (mean \pm standard deviation [SD]) in the whole study population, 54.8 ± 46.7 months in the stable, and 36.1 ± 21.4 months in the progressive group. Cases

in which the referring clinician suspected disease progression tended to be referred far more frequently, whereas cases that were clinically stable over time were referred less frequently. The between-studies interval was 8.3 ± 5.1 months in the whole study population, 14 ± 5.6 months in the stable group, and 7.8 ± 4 months in the progressive group. Statistical analysis was performed using the two-tailed t-test and percentile rankings. No verified case of radiation necrosis was observed during the period of this study.

TABLE 2
Pathological, clinical, and neuroradiological findings in 11 patients with progressive disease*

Case No.	Age (yrs), Sex	Diagnosis	Mos to Disease Onset	Mos to Treatment†	Clinical Data	MR Imaging	FDG-PET	Cho on ¹ H-MRS Imaging	% Change Cho
17	35, M	astro II	30	27 (RT)	‡	N	hypo	1.15	
		REC (III)	35	32 (RT) [Sx]	P	P, N	P, hyper	2.13	85
18	50, M	astro IV	31	31 (Sx, C, & RT)	‡	E	hypo	1.06	
		REC (IV)	34	34 (Sx, C, & RT)	S	S, E	S, hypo	1.18	11
			43	[Bx & C]	P	P, E	P, hyper	1.87	58
19	55, F	astro III	21	21 (Sx, RT, & C)	‡	E	hypo	0.63	
			32		P	P, E	S, hypo	0.92	46
20	32, F	astro I	49	31 (RT)	‡	N	hypo	1.34	
		REC (IV)	55	37 (RT)	S	N	hypo	1.09	-19
			71	[Sx & C]	P	P, N	S, hypo	2.04	87
21	30, F	astro II	56	56 (RT)	‡	E	hypo	0.88	
			60		P	P, E	S, hypo	1.67	90
22	31, M	astro IV	2	18 (Sx)	‡	N	hyper	1.30	
		REC (IV)	20	[Sx, RT, & C]	P	P, E	P, hyper	1.90	46
23	32, F	astro III	78	78 (Sx & RT)	‡	N	hypo	1.90	
		REC (III), RN	83	[Sx]	P	P, E	P, hypo	2.79	47
24	49, F	astro IV	20	30 (Sx, RT, & C)	‡	E	hypo	1.90	
			28		P	P, E	P, hyper	2.79	
25	26, F	astro IV	16	12 (Sx & RT)	‡	E	hyper	1.23	
		REC (GBM)	22	18 (RT) [Sx]	P	P, E	P, hyper	1.98	61
26	48, F	astro III	20	10 (Sx & C)	‡	E	hyper	1.95	
		REC (III)	30	20 (Sx & C) [Sx & C]	P	P, E	P, hyper	3.98	104
27	35, F	astro III	10	4 (Sx & RT)	‡	E	hypo	1.60	
			20	14 (Sx & RT)	P	P, E	P, hyper	2.44	52

* Bx = biopsy; GBM = glioblastoma multiforme; P = progressive; REC = recurrence; RN = radiation necrosis; other abbreviations as in Table 1.

† Brackets designate treatments given after ¹H-MRS imaging studies were performed.

‡ No comparison with radiological studies was performed at baseline.

Results

Figures 1 and 2 show consecutive MR and ¹H-MRS images (including NAA, Cho, CR, and LAC) obtained in two representative patients. Figure 1 depicts consecutive MR and ¹H-MRS images obtained in a patient with stable disease (Case 7). In both studies, the NAA images demonstrate a signal void relative to the contralateral hemisphere that encompasses most of the region of abnormal signal intensity on the T₂-weighted image. The Cho images show a signal enhancement relative to the contralateral hemisphere that is located in the center of the lesion depicted with T₂ weighting. The size of the area of Cho enhancement appears smaller in the second study, likely because of the slight differences in slice location or angulation. The CR image in the repeated study shows a minor area of enhancement relative to the contralateral hemisphere that was not evident in the baseline study. Also, the LAC images in both studies show peripheral areas of artifactual signal elevation caused by incomplete suppression of lipid signals arising from bone marrow and extracranial tissues. This resulted from signal that could not be assigned to LAC by using established criteria (chemical shift should show a doublet centered at 1.33 ppm) after visual inspection of spectra from these voxels (data not shown).

Figure 2 shows consecutive MR and ¹H-MRS images obtained in a patient with progressive disease (Case 22). We selected this patient specifically to illustrate the complexity and heterogeneity that can be found in ¹H-MRS

imaging in a case of recurrent brain tumor with the lowest change (46%) in normalized Cho between two consecutive studies. The repeated ¹H-MRS imaging study (Fig. 2B) demonstrates that disease progression was characterized by an increased Cho signal, as well as by an increased CR signal, a decreased NAA signal, and the presence of LAC. The NAA image shows a large area of signal void relative to the contralateral hemisphere, corresponding to most of the region of abnormal signal intensity on the T₂-weighted image. The Cho image exhibits signal enhancement in a limited area of the lesion depicted with T₂ weighting. The CR image shows a signal enhancement that coincides with the area of Cho enhancement. The LAC image shows the presence of LAC in the mesial regions of the lesion depicted with T₂ weighting. As mentioned previously, the LAC images demonstrate an artifactual signal elevation at the brain periphery in both studies. We have presented only the normalized Cho findings because the normalized NAA, CR, and LAC, as well as the within-voxel metabolite ratios (NAA/Cho, NAA/CR, Cho/CR) showed no association with the patient's categorization.

Figure 3 illustrates the percentage change in normalized Cho intensity that was observed between two consecutive studies for the two groups. In the stable group, the between-studies percentage changes of the normalized Cho were always below 35 (range -33 to +28%, mean ± SD, 0.4 ± 13.2%). In several instances, the percent age changes in normalized Cho took a negative direction. Because of the heterogeneity of previous treatments and the

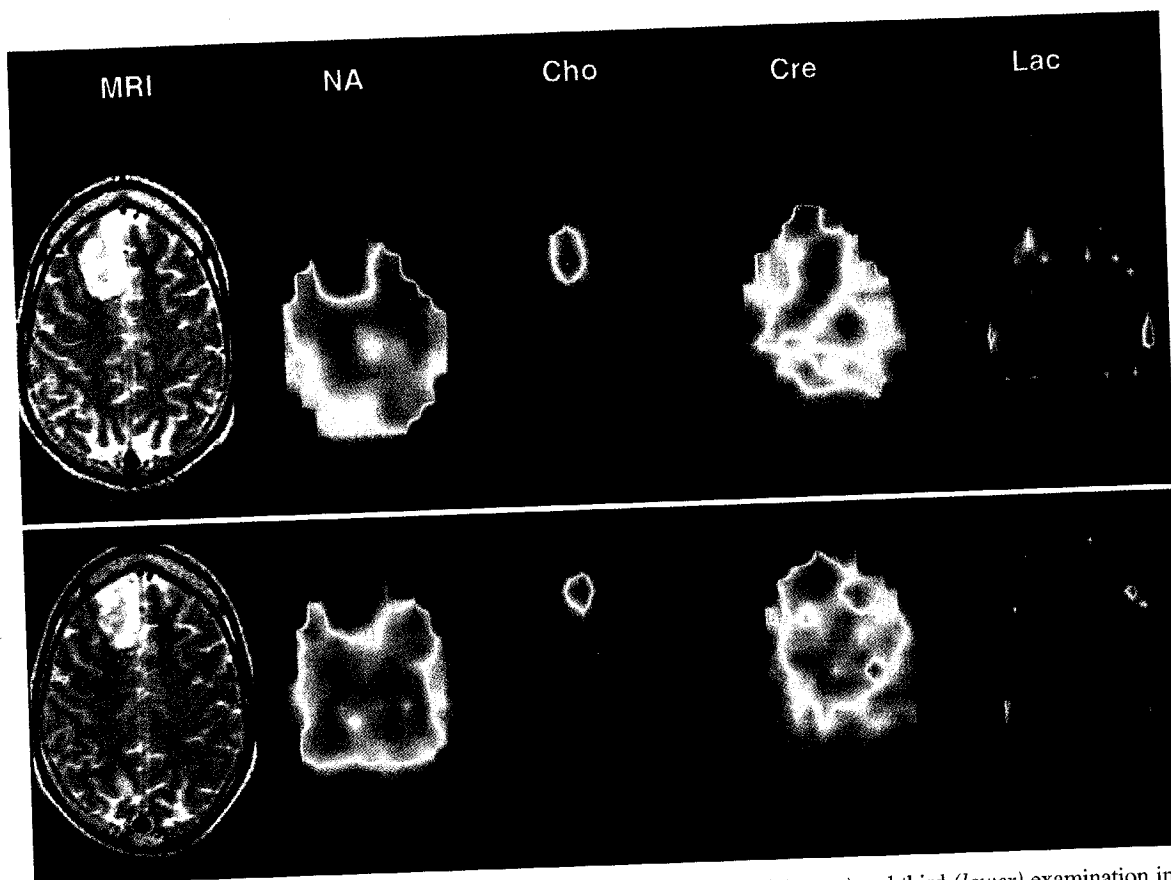


FIG. 1. Magnetic resonance and ^1H -MRS images obtained on the second (*upper*) and third (*lower*) examination in a patient with stable disease. The MR imaging slice is 3 mm thick and corresponds to the center of the 15-mm-thick ^1H -MRS imaging slice. The ^1H -MRS imaging data are displayed using a color scale that depicts the strongest signal intensity with *red* and the weakest with *dark blue*. Color images are scaled to the highest value for each metabolite signal intensity for each ^1H -MRS imaging slice, so that the pattern of regional distribution of metabolite signal intensities within the same slice can be compared between patients, although color intensity from the same anatomical location cannot be so compared. For a detailed discussion of the imaging example see the *Results* section.

differences in time from treatment in our study group, we could not discriminate possible therapy-related improvements of the disease from intraindividual variability of the ^1H -MRS imaging. In the group with progressive disease, the between-studies percentage changes in the normalized Cho were always above 45 (range 46–104%, mean \pm SD, $55.6 \pm 33.2\%$). The diagram aptly demonstrates how well the percentage change in normalized Cho intensity segregates the two groups: a critical value of 35% completely segregates them. A t-test showed a statistically significant ($p < 0.00005$) difference between the stable and progressive groups.

Patients with glioma who develop malignant degeneration or malignant recurrence are known to have a statistically poor prognosis for survival, whereas patients with stable disease (an initial low-grade diagnosis or effective treatment) have longer survival times. Hence, a survival review may indicate whether the patients were accurately categorized. A survival review performed at the end of the study showed that all but one patient (Case 11) in the group with stable disease had survived, whereas all but one patient (Case 27) in the group with progressive disease had died. This finding is consistent with expectations,

indicating that the clinical categorization at the time of imaging studies was accurate.

Discussion

Morphological studies using CT and MR imaging, and physiological imaging using PET and SPECT scanning have played a pivotal role in defining landmarks used to manage primary brain tumors clinically. However, as indicated earlier, many questions regarding the care of patients with cerebral gliomas remain unanswered. The addition of complementary biochemical information, as provided by ^1H -MRS imaging, could lead to further advances in patient management. Repeated ^1H -MRS imaging examinations provide a noninvasive method to determine whether a patient is affected by a progressive neoplasm that should be treated or is in stable condition. Undoubtedly, the widespread availability of high-field (1.5- and 2-tesla) MR imagers will help make this procedure available to and accepted by those physicians who manage cases of primary brain tumors.

In this study, MR imaging and FDG-PET together with the neurological examination and the biopsy findings

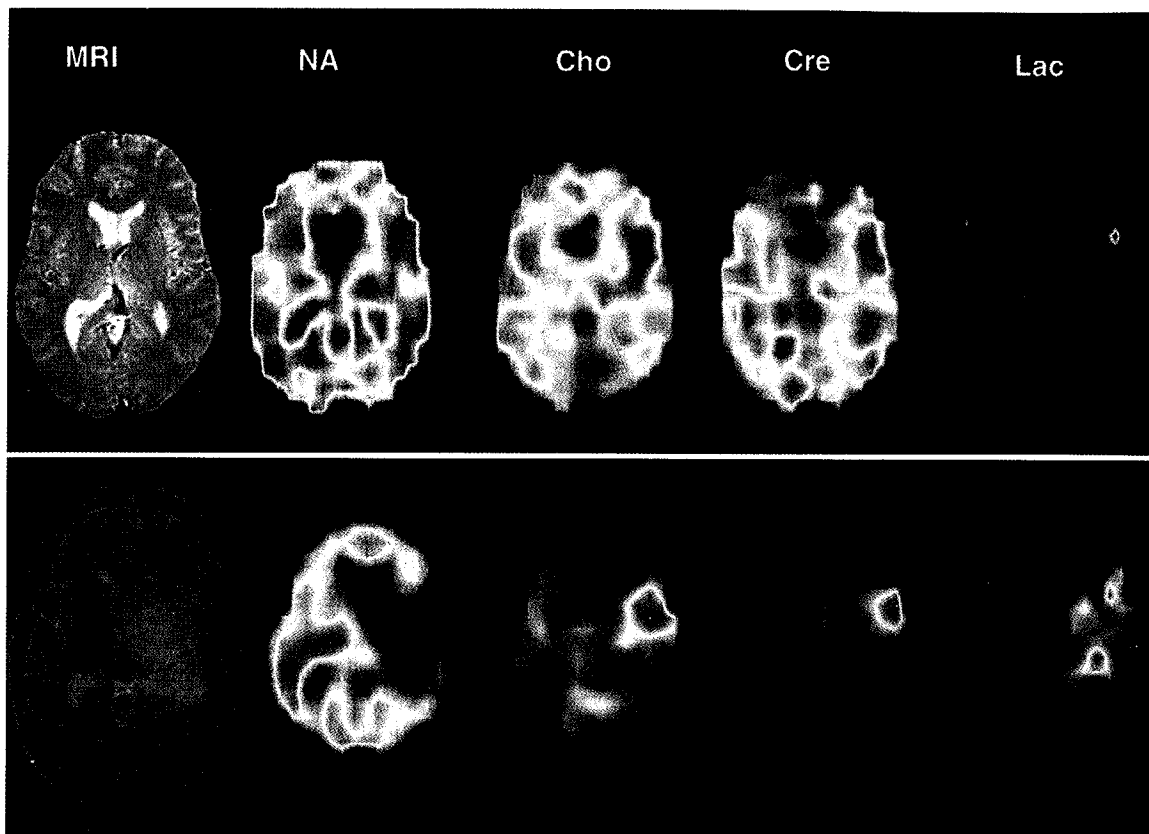


FIG. 2. Magnetic resonance and ^1H -MRS images obtained on the first (*upper*) and second (*lower*) examination in a patient with progressive disease showing the lowest between-studies change in normalized Cho. For color scales, see Fig. 1. For a detailed discussion of the imaging example see the *Results* section.

(in seven of 11 progressive cases) were used to establish whether a particular patient was exhibiting a malignant degeneration. Our results indicate that serial ^1H -MRS imaging effectively and accurately differentiates between stable and progressive disease. The ^1H -MRS imaging data not only show a difference in distribution (means) between the two groups, but also a high discriminatory power, in that any threshold between 35% and 45% of between-study percentage change in normalized Cho yields separation between stable and progressive cases.

The ^1H -MRS imaging method has two major limitations that account for the high rate (approximately 30%) of technically inadequate studies. First, the metabolite signals from some regions (for example, posterior fossa, medial temporal lobes, and superior medial gyri) are broadened by partial magnetic field inhomogeneities caused by the proximity of sinuses and bones. Second, the signal/noise ratio can be affected by head motion during the acquisition phase.

Establishing which compounds contribute to the Cho signal has been an area of active research in recent years. If the major water-soluble Cho-containing compounds in the brain are added together, their total concentration does not account for the large signal that is seen in vivo. This has led to the conclusion that relatively immobile lipid molecules, such as phosphatidylcholine, can be seen in vivo.³⁴ Conversely, in a 1994 in vivo and in vitro study of

the canine brain, the Cho signal was attributed predominantly to water-soluble glycerophosphocholine and phosphocholine.⁵ A recent report on 18 patients with neoplastic and infectious brain lesions stated that the in vivo Cho signal correlated with in vitro measures of cellular density and water-soluble Cho-containing compounds (free Cho, phosphocholine and glycerophosphocholine), but not with membrane-bound phosphatidylcholine.³⁵ All these Cho-containing compounds participate in phospholipid metabolism. Thus, the increased Cho peak found in most of the ^1H -MRS and ^1H -MRS imaging studies of brain tumors has been attributed to a greater membrane synthesis, increased cellularity, or to a rapid cell turnover. Our observations are consistent with these views. An increase in Cho paralleling clinical deterioration is consistent with increased cellularity, as well as with increased cell turnover and phospholipid metabolites.

In this study, the criterion for ROI selection was unique. We hypothesized that the "hottest" Cho region represents the site of highest tumor malignancy. Until now, investigators have used average readings over the entire tumor volume.^{19,43} The "worst" voxel analysis method we used is analogous to the pathological examination, in which the diagnosis is derived from the worst area of the biopsy specimen. This seemed logical despite the large difference between histopathological and ^1H -MRS imaging resolution. The promising results of this study support the valid-

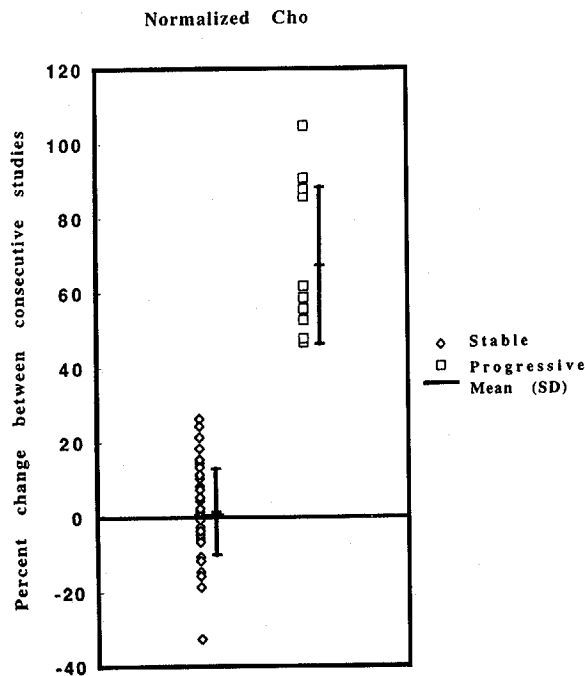


FIG. 3. Scatterplot showing percentage change in normalized Cho signal intensity that was seen between two consecutive studies for the two groups of patients.

ity of analyzing the worst voxel. Moreover, results reveal how $^1\text{H-MRS}$ imaging might be used to identify regions to be sampled by means of stereotactic biopsy or regions suitable for focal therapy.

The NAA molecule is thought to be neuron specific,^{36,54} and it is reduced or absent in tumors of glial cell origin.^{2,3,6,7,16,19,21,27,30,37,38,42,43,46,48,50,55} In our study, the reduced NAA signal did not allow us to discriminate between the stable and progressive disease groups. This result is consistent with the destructive and infiltrative nature of gliomas. Once the tumor cells have replaced the normal neurons, no further NAA reduction can be correlated with additional tumor progression.

The CR signal measures both creatine and phosphocreatine metabolites involved in cellular energy metabolism.³⁴ In a previous study,³⁷ the CR peak was increased in some tumors. We found similar evidence (one example is shown in Fig. 2), with the CR signal from the tumor increasing in 44% of the total patient population; however, the signal did not allow us to discriminate between the two groups of patients.

The LAC signal rises whenever the LAC-producing anaerobic glycolytic pathway exceeds the capacity of the LAC-catabolizing respiratory pathways, or when the cellular capacity for exporting LAC to the bloodstream is impaired.⁴⁴ The presence of LAC in brain tumors has been highlighted by several groups of authors,^{2,3,19,21,48} and, although LAC is more likely to be found in high-grade gliomas, its importance as a potential predictor of malignancy is still being debated.^{2,19,48} This may be associated, in part, with the difficulty of separating the LAC signals from those of lipids and macromolecules that are either within the tumor or that contaminate the tumor spectrum because

of incomplete volumetric localization. In the present study, LAC was occasionally found in some high-grade tumors (Fig. 2), but its presence and changes between examinations did not help us differentiate between the two groups of patients.

In the present analysis the metabolite signal intensities were measured in the tumor and in the healthy contralateral brain to form between-voxel ratios. In addition, within-voxel metabolite signal intensity ratios (NAA/Cho, NAA/CR, Cho/CR) for each ROI were determined. We believe that the absence of significant results when the within-voxel ratio is used reflects the limitations of estimating metabolite changes by ratios when a simultaneous change of two or more metabolites occurs. This could also be related to the limited value of NAA and CR to differentiate between the two groups of patients. The use of between-voxel ratios, which proved to be the most informative, is validated by our previous work, in which we demonstrated that in healthy adults there are no statistically significant side-to-side differences for any of the reported metabolites.^{52,53}

With this study we could not answer the very relevant question of the differential diagnosis between radiation necrosis and tumor recurrence, simply because we lacked cases with verified, pure radiation necrosis. We encountered one patient (Case 23) in whom a biopsy showed the coexistence of tumor recurrence and radiation necrosis. The differential diagnosis could be formulated only at the microscopic level, which is beyond the resolution of $^1\text{H-MRS}$ imaging.

Conclusions

This study shows that serial $^1\text{H-MRS}$ imaging can be used to detect glioma progression. We anticipate that this noninvasive method may play a role in improving the management of patients with cerebral gliomas.

Acknowledgments

We thank A. S. Barnett for developing and making available the $^1\text{H-MRS}$ imaging data processing, G. Campbell for his help in performing the statistical analysis, and D. G. Schoenberg for skillful editing.

References

1. Alavi JB, Alavi A, Chawluk J, et al: Positron emission tomography in patients with glioma. A predictor of prognosis. *Cancer* **62**:1074-1078, 1988
2. Alger JR, Frank, JA, Bizzi A, et al: Metabolism of human gliomas: assessment with H-1 MR spectroscopy and F-18 fluorodeoxyglucose PET. *Radiology* **177**:633-641, 1990
3. Arnold DL, Shoubridge EA, Villemure JG, et al: Proton and phosphorus magnetic resonance spectroscopy of human astrocytomas *in vivo*. Preliminary observations on tumor grading. *NMR Biomed* **3**:184-189, 1990
4. Barker FG II, Chang SM, Valk PE, et al: 18-Fluorodeoxyglucose uptake and survival of patients with suspected recurrent malignant glioma. *Cancer* **79**:115-126, 1997
5. Barker PB, Breiter SN, Soher BJ, et al: Quantitative proton spectroscopy of canine brain: *in vivo* and *in vitro* correlations. *Magn Reson Med* **32**:157-163, 1994
6. Bizzi A, Movsas B, Tedeschi G, et al: Response of non-Hodgkin lymphoma to radiation therapy: early and long-term assess-

Serial MRS in gliomas

- ment with H-1 MR spectroscopic imaging. **Radiology** **194**:271-276, 1995
7. Bruhn H, Frahm J, Gyngell ML, et al: Noninvasive differentiation of tumors with use of localized H-1 MR spectroscopy *in vivo*: initial experience in patients with cerebral tumors. **Radiology** **172**:541-548, 1989
 8. Cairncross JG, Laperriere NJ: Low-grade glioma. To treat or not to treat? **Arch Neurol** **46**:1238-1239, 1987
 9. Coleman RE, Hoffman JM, Hanson MW, et al: Clinical application of PET for the evaluation of brain tumors. **J Nucl Med** **32**:616-622, 1991
 10. Davis WK, Boyko OB, Hoffman JM, et al: [¹⁸F]2-fluoro-2-deoxyglucose-positron emission tomography correlation of gadolinium-enhanced MR imaging of central nervous system neoplasia. **AJNR** **14**:515-523, 1993
 11. Di Chiro G: Positron emission tomography using [¹⁸F]fluorodeoxyglucose in brain tumors. A powerful diagnostic and prognostic tool. **Invest Radiol** **22**:360-371, 1987
 12. Di Chiro G: Which PET radiopharmaceutical for brain tumors? **J Nucl Med** **32**:1346-1348, 1991
 13. Di Chiro G, DeLaPaz RL, Brooks RA, et al: Glucose utilization of cerebral gliomas measured by [¹⁸F] fluorodeoxyglucose and positron emission tomography. **Neurology** **32**:1323-1329, 1982
 14. Di Chiro G, Oldfield E, Wright DC, et al: Cerebral necrosis after radiation and/or intraarterial chemotherapy for brain tumors: PET and neuropathologic studies. **AJR** **150**:189-197, 1988
 15. Doyle WK, Budinger TF, Valk PE, et al: Differentiation of cerebral radiation necrosis from tumor recurrence by [¹⁸F]FDG and ⁸²Rb positron emission tomography. **J Comput Assist Tomogr** **11**:563-570, 1987
 16. Duyn JH, Gillen J, Sobering G, et al: Multisection proton MR spectroscopic imaging of the brain. **Radiology** **188**:277-282, 1993
 17. Francavilla TL, Miletich RS, Di Chiro G, et al: Positron emission tomography in the detection of malignant degeneration of low-grade gliomas. **Neurosurgery** **24**:1-5, 1989
 18. Fulham MJ: PET with [¹⁸F]fluorodeoxyglucose (PET-FDG): an indispensable tool in the proper management of brain tumors, in Hubner KF, Coolmann J, Buonocore E, et al (eds): **Clinical Positron Emission Tomography**. St. Louis: Mosby Year Book, 1992, pp 50-60
 19. Fulham MJ, Bizzi A, Dietz MJ, et al: Mapping of brain tumor metabolites with proton MR spectroscopic imaging: clinical relevance. **Radiology** **185**:675-686, 1992
 20. Fulham MJ, Di Chiro G: Neurologic PET and SPECT, in Harbert T, Eckelman W, Neumann R (eds): **Textbook of Nuclear Medicine**. Basel: Thieme, 1996, pp 361-385
 21. Gill SS, Thomas DGT, Van Bruggen N, et al: Proton MR spectroscopy of intracranial tumors: *in vivo* and *in vitro* studies. **J Comput Assist Tomogr** **14**:497-504, 1990
 22. Glantz MJ, Hoffman JM, Coleman RE, et al: Identification of early recurrence of primary central nervous system tumors by [¹⁸F]fluorodeoxyglucose positron emission tomography. **Ann Neurol** **29**:347-355, 1991
 23. Hanson MW, Glantz MJ, Hoffman JM, et al: FDG-PET in the selection of brain lesions for biopsy. **J Comput Assist Tomogr** **15**:796-801, 1991
 24. Herholz K, Heindel W, Luyten PR, et al: *In vivo* imaging of glucose consumption and lactate concentration in human gliomas. **Ann Neurol** **31**:319-327, 1992
 25. Herholz K, Pietrzyk U, Voges J, et al: Correlation of glucose consumption and tumor cell density in astrocytomas. A stereotactic PET study. **J Neurosurg** **79**:853-858, 1993
 26. Hölzer T, Herholz K, Jeske J, et al: FDG-PET as a prognostic indicator in radiochemotherapy of glioblastoma. **J Comput Assist Tomogr** **17**:681-687, 1993
 27. Jackson EF: *In vivo* magnetic resonance spectroscopy in humans: a brief review. **Am J Physiol Imaging** **7**:146-154, 1992
 28. Jaecle KA: Clinical presentation and therapy of nervous system tumors, in Bradley WG, Daroff RB, Fenichel GM, et al (eds): **Neurology in Clinical Practice: Principles of Diagnosis and Management**, ed 1. Boston: Butterworth-Heimann, 1991, Vol 2, pp 1008-1030
 29. Kondziolka D, Lunsford LD, Martinez AJ: Unreliability of contemporary neurodiagnostic imaging in evaluating suspected adult supratentorial (low-grade) astrocytoma. **J Neurosurg** **79**:533-536, 1993
 30. Kugel H, Heindel W, Ernestus RI, et al: Human brain tumors: spectral patterns detected with localized H-1 MR spectroscopy. **Radiology** **183**:701-709, 1992
 31. Laws ER Jr, Taylor WF, Clifton MB, et al: Neurosurgical management of low-grade astrocytoma of the cerebral hemispheres. **J Neurosurg** **61**:665-673, 1984
 32. Levivier M, Goldman S, Pirotte B, et al: Diagnostic yield of stereotactic brain biopsy guided by positron emission tomography with [¹⁸F]fluorodeoxyglucose. **J Neurosurg** **82**:445-452, 1995
 33. Macdonald DR, Cascino TL, Schold SC Jr, et al: Response criteria for Phase II studies of supratentorial malignant glioma. **J Clin Oncol** **8**:1277-1280, 1990
 34. Miller BL: A review of chemical issues in ¹H NMR spectroscopy: N-acetyl-aspartate, creatine and choline. **NMR Biomed** **4**:47-52, 1991
 35. Miller BL, Chang L, Booth R, et al: *In vivo* ¹H-MRS choline: correlation with *in vitro* chemistry/histology. **Life Sci** **58**:1929-1935, 1996
 36. Moffett JR, Nambodiri MAA, Neale JH: Enhanced carbodiimide fixation for immunohistochemistry: application to the comparative distributions of N-acetylaspartylglutamate and N-acetylaspartate immunoreactivities in rat brain. **J Histochem Cytochem** **41**:559-570, 1993
 37. Negendank WG, Sauter R, Brown TR, et al: Proton magnetic resonance spectroscopy in patients with glial tumors: a multicenter study. **J Neurosurg** **84**:449-458, 1996
 38. Ott D, Hennig J, Ernst T: Human brain tumors: assessment with *in vivo* proton MR spectroscopy. **Radiology** **186**:745-752, 1993
 39. Patronas NJ, Di Chiro G, Brooks RA, et al: Work in progress: [¹⁸F]fluorodeoxyglucose and positron emission tomography in the evaluation of radiation necrosis of the brain. **Radiology** **144**:885-889, 1982
 40. Patronas NJ, Di Chiro G, Kufra C, et al: Prediction of survival in glioma patients by means of positron emission tomography. **J Neurosurg** **62**:816-822, 1985
 41. Piepmeier JM: Observations on the current treatment of low-grade astrocytic tumors of the cerebral hemispheres. **J Neurosurg** **67**:177-181, 1987
 42. Poptani H, Gupta RK, Roy R, et al: Characterization of intracranial mass lesions with *in vivo* proton MR spectroscopy. **AJNR** **16**:1593-1603, 1995
 43. Preul MC, Caramanos Z, Collins DL, et al: Accurate, noninvasive diagnosis of human brain tumors by using proton magnetic resonance spectroscopy. **Nature Med** **2**:323-325, 1996
 44. Prichard JW: What the clinician can learn from MRS lactate measurement. **NMR Biomed** **4**:99-102, 1991
 45. Report of the Therapeutics and Technology Assessment Subcommittee of the American Academy of Neurology: Assessment: positron emission tomography. **Neurology** **41**:163-167, 1991
 46. Ross B, Michaelis T: Clinical applications of magnetic resonance spectroscopy. **Magn Reson Q** **10**:191-247, 1994
 47. Schifter T, Hoffman JM, Hanson MW, et al: Serial FDG-PET studies in the prediction of survival in patients with primary brain tumors. **J Comput Assist Tomogr** **17**:509-516, 1993
 48. Segebarth CM, Balériaux DF, Luyten PR, et al: Detection of metabolic heterogeneity of human intracranial tumors *in vivo*

- by ^1H NMR spectroscopic imaging. **Magn Reson Med** **13**: 62-76, 1990
49. Shapiro WR, Shapiro JR: Primary brain tumors, in Asbury AK, McKhann GM, McDonald WI (eds): **Diseases of the Nervous System: Clinical Neurobiology**, ed 2. Philadelphia: WB Saunders, 1992, Vol 2, pp 1074-1092
 50. Sutton LN, Wehrli SL, Gennarelli L, et al: High-resolution ^1H -magnetic resonance spectroscopy of pediatric posterior fossa tumors *in vitro*. **J Neurosurg** **81**:443-448, 1994
 51. Taveras JM, Thompson HG Jr, Pool JL: Should we treat glioblastoma multiforme? A study of survival in 425 cases. **AJR** **87**:473-479, 1962
 52. Tedeschi G, Bertolino A, Campbell G, et al: Reproducibility of proton MR spectroscopic imaging findings. **AJNR** **17**: 1871-1879, 1996
 53. Tedeschi G, Bertolino A, Righini A, et al: Brain regional distribution pattern of metabolite signal intensities in young adults by proton magnetic resonance spectroscopic imaging. **Neurology** **45**:1384-1391, 1995
 54. Urenjak J, Williams SR, Gadian DG, et al: Proton nuclear magnetic resonance spectroscopy unambiguously identifies different neural cell types. **J Neurosci** **13**:981-989, 1993
 55. Usenius JPR, Kauppinen RA, Vainio PA, et al: Quantitative metabolite patterns of human brain tumors: detection by ^1H NMR spectroscopy *in vivo* and *in vitro*. **J Comput Assist Tomogr** **18**:705-713, 1994
 56. Valk PE, Budinger TF, Levin VA, et al: PET of malignant cerebral tumors after interstitial brachytherapy. Demonstration of metabolic activity and correlation with clinical outcome. **J Neurosurg** **69**:830-838, 1988
 57. Zimmerman RA: Imaging of adult central nervous system primary malignant gliomas. Staging and follow-up. **Cancer** **67**: 1278-1283, 1991

Manuscript received February 20, 1997.

Accepted in final form May 16, 1997.

Dr. Lundbom is on leave of absence from the University Hospital of Turku, Turku, Finland.

Address reprint requests to: Gioacchino Tedeschi, M.D., Neuroimaging Branch, NINDS, NIH, Building 10, Room 1C227, 9002 Rockville Pike, Bethesda, Maryland 20892.